

## Soil Displacements due to Tunneling in Dense Silty Sand Layer Underneath Bridge Pile Foundation in Bangkok

Wanchai TEPARAKSA<sup>1</sup>, Suktay LIM<sup>2</sup>, and Satoru SHIBUYA<sup>3</sup>

<sup>1</sup>Associate Professor, <sup>2</sup>Doctoral Candidate, <sup>3</sup>Professor

<sup>1,2</sup>Department of Civil Engineering, Chulalongkorn University, Bangkok 10330, Thailand

Mobile: (+66) 818 441322, Tel: (+66) 2 218 6575, Fax: (+66) 2 251 7304

Email: wanchai.te@chula.ac.th, suktay\_lim@yahoo.fr

<sup>3</sup>Department of Architecture and Civil Engineering, Kobe University, 657-8501 Japan

Tel: (+81) 78 803 6023, Fax: (+81) 78 803 6023, Email: sshibuya@kobe-u.ac.jp

### Abstract

A tunnel was bored by means of EPB shield in dense silty sand layer about 27.5 m below ground surface in Bangkok. The main route of the monitored tunnel is located underneath a bridge and busy roads. Several factors including soil parameters, surcharges, and obstructions play an important role in obtaining an accurate estimation of soil movements in response to tunneling. This research aims to demonstrate the use of elastoplastic failure criteria of Mohr Coulomb soil model to back-simulate the ground surface and subsurface settlements. The two-dimensional (2D) numerical analyses were carried out to confirm the design assumptions, Young Modulus. The settlements yielded by the numerical method were similar to the field monitored data at both ground surface and subsurface. The results based on empirical method for surface settlements were also acceptable. In short, the back-simulation and analysis of this study and those of the previous projects of tunneling provide an accurate prediction for future tunnel excavation with similar geological conditions.

**Keywords:** Tunneling, Soil movements, Numerical simulation, Obstructions.

### 1. Introduction

The tunnel has been excavated underneath the busy roads and some underground obstructions such as bridge pile foundations. Funded by the Bangkok Metropolitan Authority (BMA), the second shortcut flood-diversion tunnels (SFDT) was designed and under construction in order to

alleviate flooding in Bangkok. This SFDT (Outer Diameter, OD = 5.55 m) is about 5 km long and will collect floodwater from the Saensaep and Latphroa canals and divert to the Phrakhanong pumping station. The intake shaft is located at the junction of the Saensaep and Latphroa canals while the outlet shaft and pumping station are near the Phrakhanong canal connected directly to the Chaophraya River (Fig.1).



Fig. 1 Location of BMA flood diversion tunnel project (Saenseap Latproa-Phrakhanong)

An Earth Pressure Balance (EPB) shield machine, OD = 5.70 m and 8.05 m in length, is used for tunneling the whole project. In order to verify the risk potential, the numerical analysis had been performed to simulate the tunneling performance in terms of ground surface and subsurface displacements as well as bridge structure and building settlements. Moreover, the field instrumentation records and the recorded data from control panel of Tunnel Boring Machine (TBM) during the operation are collected to study the behaviors of ground displacements

responding to EPB excavation. Only Klongtan Bridge area where the most comprehensive monitoring system for this project was implemented is selected for this study (Fig. 2).

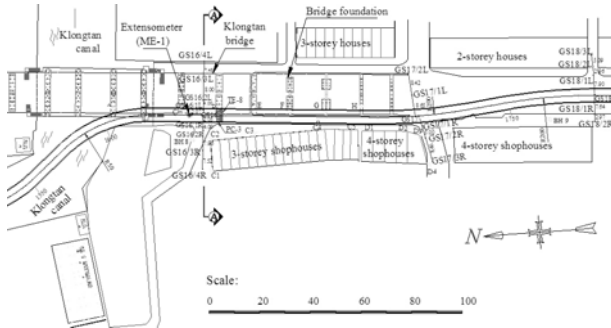


Fig. 2 Selected studied area

Based on Finite Element Method (FEM) program, the back analyses and simulation are carried out to obtain the appropriate design parameter of Young Modulus. The elasto-plastic failure criteria of Mohr Coulomb soil model are employed for the 2D simulation since they have been used in several research studies related to the underground constructions in Bangkok and other countries [2, 8-11]. Although this soil model is suitable for most designs of underground structures, the designers should have enough practical experiences related to these works.

**2. Geology at the Site and Tunnel Properties**

The Geology of Bangkok is typically alluvial flood plain of the Chaophraya river. The subsoil profile is relatively uniform throughout the whole city area [7] including along the SFDT. The subsoil profile within the studied area is presented in Fig. 3. At this section, the tunnel was fully excavated in dense silty sand layer. An old Klongtan bridge was found at this selected area, and the tunnel was bored about 3 m. below the tips of the piles (Fig. 3).

Moreover, an unusual geological condition of Bangkok is the pore water pressure. It is generally hydrostatic starting from one meter below the ground level. Due to deep well pumping from the aquifer, it has led

to under-drainage of the soft and the first stiff clay layers [8, 12]. That is why the piezometric level of the Bangkok aquifer is reduced but quite constant at about 23 m below ground surface (Fig. 4). Teparaksa and Heidengren (1999) stated that “this low piezometric level contributes to the increase in effective stress, causing ground subsidence in this city”.

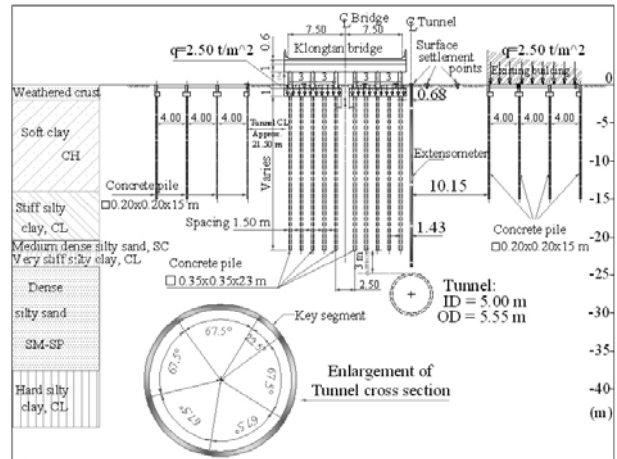


Fig. 3 Subsoil profile (section AA)

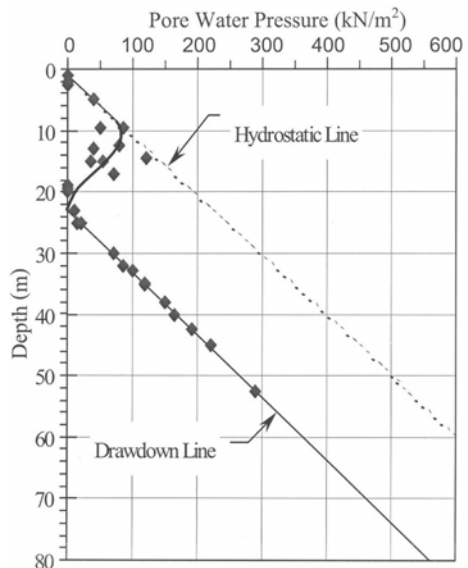


Fig. 4 Ground water pressure of Bangkok [8]

The tunnel lining consists of pre-cast bolted reinforced concrete, 400 ksc of compression strength, having six segments per ring in which one is called key segment (Fig.3). Each segment is 0.275 m thick and 1.2 m. wide for straight alignment, but this width is reduced to 0.6 m for curvature. The water sealing

material named Hydrotite (RS type) is used to prevent the leakage of water at each joint.

### 3. Constitutive Soil Model and Numerical Simulation

The finite element program called PLAXIS 2D [1] was mainly used in this research. The plane strain and 15-node triangular element, which consists of 15 nodes and 12 stress points, are set to model the deformations and stresses in the soil. However, the structure components, which are the foundations, will be simulated as the line elements based on elastic properties.

#### 3.1 Constitutive Soil Model

The constitutive soil model based on elasto-plastic failure criteria of Mohr-Coulomb was considered in this research. This soil model is most appropriate when soil data are not sufficient and for a preliminary analysis of the problem. The reason for this is this model is simple and practical. It is stated in the manuals of PLAXIS program that, “This robust and simple *non-linear model* is based on soil parameters that are known in most practical situations, which lead to a quick and simple analysis; moreover, the procedure tends to reduce errors” [1].

As the major ground displacement response to bored tunnel occurred in the short-term condition [5, 9], the undrained analyses based on undrained soil parameters were appropriate for the cohesive soil layers. Thus, the effect of ground water flow and consolidation was not considered in the model.

Mair (1993) reported the changes of soil stiffness with different working shear strain levels for various underground structures as shown in Fig. 5. The typical working range of tunnels is between 0.1 and 1%.

The relationships between shear strain and the ratio of in-situ secant shear modulus ( $G_{sec(in-situ)}$ ) to undrained shear strength obtained from monotonic undrained triaxial compression ( $S_{u(MTX)}$ ) and field vane shear tests ( $S_{u(FVS)}$ ) for Bangkok clay were established [6] (Fig. 6). The average values of  $G_{sec(in-situ)}/S_{u(MTX)}$  in soft clay corresponding to 0.1 and

1% of shear strain were about 230 and 70 respectively while  $G_{sec(in-situ)}/S_{u(FVS)}$  were about 315 and 80 (Fig. 6). However, these average values in stiff clay were found about 530 and 100 for both  $G_{sec(in-situ)}/S_{u(MTX)}$  and  $G_{sec(in-situ)}/S_{u(FVS)}$ .

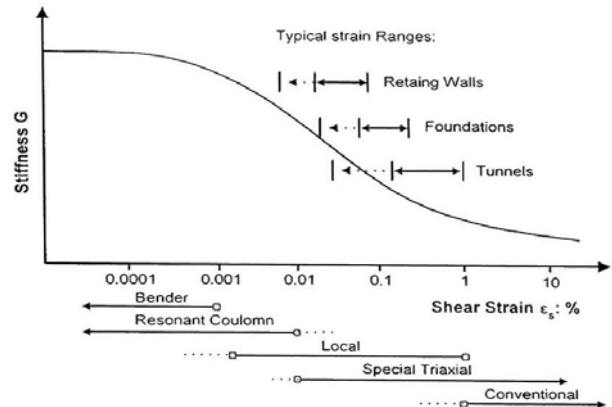


Fig. 5. Shear modulus and working shear strains for underground structures [3]

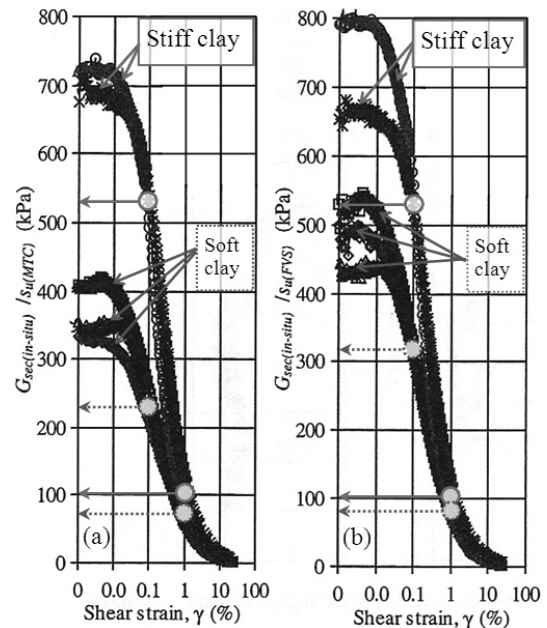


Fig. 6 Variations of  $G_{sec(in-situ)}/S_u$  with shear strains, (a)  $S_u$  from MTX and (b)  $S_u$  from field vane shear tests [6]

For the undrained shear condition of clay sample, the secant shear modulus ( $G_{sec}$ ) linked to the secant young modulus ( $E_{sec}$ ) by the relation  $G_{sec} = E_{sec}/3$ . Thus, the average values of  $E_u/S_u$  in soft clay corresponding to

0.1 and 1% shear strain were about 690 and 210 respectively for triaxial tests; however, these values slightly increased to 945 and 240 for field vane shear tests. Moreover, these ratios became 1590 and 300 for stiff clay layer.

Within the range of shear strain 0.1 and 1%, Teparaksa and Heidengren, (1999) carried out the back analysis based on 2D FEM program with Mohr-Coulomb soil model, and found that the appropriate Young Modulus ratios ( $E_u/S_u$ ) for estimating the ground displacements due to EPB shield tunneling in Bangkok were 240 and 480 for soft and stiff clays, respectively. These ratios are in the same intervals as what yielded from laboratory and in-situ tests described previously. In addition, Teparaksa [9] used the values of drained modulus  $E'$  ( $\text{kN/m}^2$ ) =  $2000.N_{60}$  ( $N_{60}$  is the SPT  $N$ -value at 60% Energy Ratio) for silty sand to design a tunnel bored in Bangkok subsoils. Therefore, for the soil stiffness,  $E_u/S_u$  and  $E'$ , 240 and 480 for soft and stiff clays respectively, and  $2000.N_{60}$ , are used in this paper. Table 1 presents the soil parameters used in the FEM simulation.

Table 1 Soil parameters for FEM analyses

| Depth (m)   | Soil layer                  | $\gamma$ ( $\text{kN/m}^3$ ) | $S_{u(FVS)}$ , $S_u$ ( $\text{kN/m}^2$ ) | $\phi$ ( $^\circ$ ) | $E_u$ , $E'$ ( $\text{kN/m}^2$ ) | $\nu$ (-) | $K_o$ , $K$ |
|-------------|-----------------------------|------------------------------|--|---------------------|----------------------------------|-----------|-------------|
| 0.00-2.00   | Weathered crust             | 17.50                        | 30.00                                    | -                   | 10800                            | 0.350     | 0.650       |
| 2.00-14.00  | Soft clay, CH               | 15.70                        | 24.00                                    | -                   | 5760                             | 0.495     | 0.837       |
| 14.00-20.50 | Stiff silty clay, CL        | 19.00                        | 80.60                                    | -                   | 38688                            | 0.495     | 0.620       |
| 20.50-22.00 | Medium dense silty sand, SC | 20.00                        | -  | 30                  | 33354                            | 0.350     | 0.500       |
| 22.00-24.00 | Very stiff silty clay, CL   | 20.00                        | 135.00                                   | -                   | 64800                            | 0.495     | 0.561       |
| 24.00-37.50 | Dense silty sand, SM-SP     | 20.00                        | -  | 35                  | 70632                            | 0.350     | 0.426       |
| 37.50-40.00 | Hard silty clay, CL         | 20.50                        | 221.00                                   | -                   | 106080                           | 0.495     | 0.656       |

### 3.2 Numerical Simulation of Tunnel Excavation Sequence

The 2D FEM simulation of tunnel construction by means of EPB shield machine could be performed in four phases:

1. *Initial condition determination:* The initial conditions are described with initial in situ stress state and the initial

configuration, and initial water pressures. The computation of initial conditions is done after the finite element mesh has been generated. The water pressures are easily generated based on the phreatic level while the initial stresses are calculated based on the  $K_o$ -procedure for the silty sand layers and on the coefficient of total lateral earth pressure ( $K$ ) for clay and silty clay layers.

2. *The deformation and stresses induced by the existing structures and surcharges:* The deformation and stress state within the soil mass in this phase is calculated immediately after the initial conditions by activating all the existing structures and surcharges at the section under an analysis. Actually this phase is also a part of initial field conditions, which already exist on the site before the tunnel construction. Therefore the displacements happening during this phase are reset to zero for the next calculation phase. One could activate the existing structures and surcharges in two phases separately without any effect on the final deformation.
3. *The tunnel excavation and installation of precast concrete segmental linings:* The tunnel excavation and installation of precast concrete segmental linings are simulated by deactivating the soil clusters inside the tunnel and activating the segmental linings, which have been created in the input of the model. In addition, the changes of water pressures inside the tunnel are also calculated.
4. *The simulation of ground loss after passing of EPB:* The simulation of ground loss or contraction is done after the EPB shield machine passes. This ground loss is the result of several factors which are the over-cutting, different diameter of TBM and the permanent tunnel lining, and redistribution of stress in the soil mass surrounding the tunnel.

As the site conditions of the tunnel are not symmetric, the full tunnel cross sections were considered in the analyses. The finite element mesh is shown in Fig. 7.

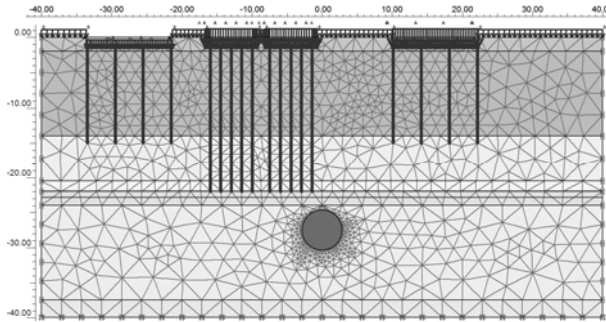


Fig. 7. Finite element mesh used in FEM simulation (section AA)

#### 4. Empirical Method of Surface Settlement

The ground surface settlement profile could be also estimated by using the following empirical approach [4]:

$$s = s_{\max} \cdot \exp\left(\frac{-x^2}{2i^2}\right) \quad (1)$$

where  $s_{\max}$  is the maximum settlement (at  $x = 0$ ) and the inflection on the settlement trough  $i$  is the value of  $x$  at the point of inflection.

The volume of the surface settlement trough per unit length can be integrated easily from Eq.1 as:

$$V_s = \sqrt{2\pi} \cdot i \cdot s_{\max} \quad (2)$$

where  $V_s$  is the volume of the surface settlement trough per unit length. Accordingly, the volume of ground loss can be yielded in a percentage of the volume of the surface settlement trough divided by the excavated volume of the tunnel:

$$V_L = \frac{4 \cdot V_s}{\pi \cdot D^2} = \frac{3.192 \cdot i \cdot s_{\max}}{D^2} \quad (3)$$

where  $V_L$  is the volume of ground loss, and  $D$  is the excavated diameter of the tunnel.

Based on the initially collected surface settlement data, the  $V_s$  was estimated. Thus, the parameters  $V_L$  and  $i$  were determined from Eq.3 and the settlement curves were plotted by using Eq.1. Furthermore, the previously computed ground loss was used as the tunnel contraction for FEM analysis. The empirical method is also used as a comparison to FEM analysis and measured data from the field.

### 5. Monitored and Computed Soil Movements

#### 5.1 Surface and Subsurface Movements

The behaviors of the recorded surface and subsurface deformation in response to tunnel excavation could be classified into 3 phases (Figs. 8): deformation in front of shield face, deformation within the length of shield body when the cutting face has been passed and the deformation behind the shield which consists of tail void deformation and subsequent settlement.

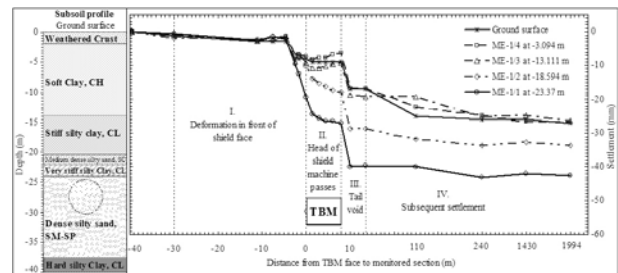


Fig. 8 Surface and subsurface movements at Extensometer ME-1

The gradual settlements are already occurred before the arrival of the shield, and these settlements are rapidly increasing when the shield approaches close to the controlled section. The vertical displacements slightly appear again for the whole shield body, and then a brutal settlement at the tail of the shield shows and remains constant during the tail void grouting. The settlements of all the layers seem constant after about one week when the TBM passes the monitored section (110 m., Fig. 8).

It is noticeable that the ground settlements corresponding to the positions of the face and tail of the TBM accelerate with average settlements about 42% and 77%,

respectively, of the total settlement measured after three months. Furthermore, this magnitude of settlement one week after the pass of the TBM reaches to 90% of the settlement after three months, which could be considered as the final short-term settlement.

The significant settlement was observed that takes place at the specific positions of the shield, face and tail, especially for the subsoil layer which is in the zone of one diameter above the crown of the tunnel (ME-1/1 in Figs. 8). It is probably a sensitive area.

**5.2 Surface Settlement Profile**

By reproducing the settlement trough based on the empirical method (Eq.1 and 3), the  $V_L$  was 1.79% for both monitored sections (GS16 and GS18 in Fig. 9).

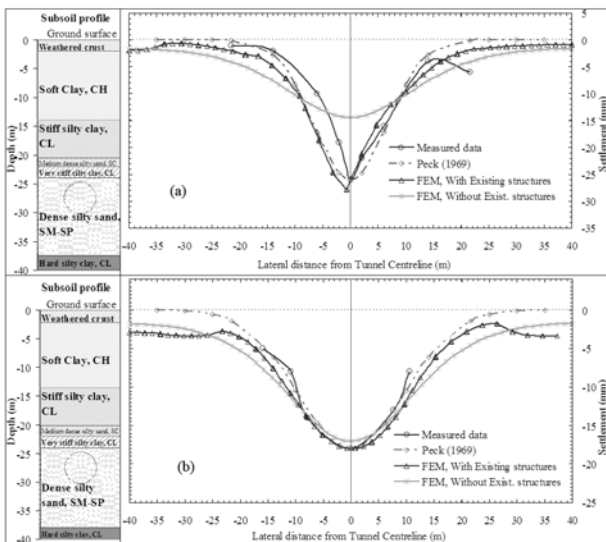


Fig. 9 Surface settlements monitored at (a) GS16 and (b) GS18

The figures show a good agreement among empirical and FEM results and the measured data (obtained three-month after TBM passed). The values of  $i$  are  $0.24Z_0$  and  $0.35Z_0$  for events as in Figs. 9a and 9b respectively and where  $Z_0$  is the depth from the ground surface to the tunnel axis.

When building structures are added as a parameter, the results of the surface settlements are strongly influenced as shown in Fig.9. Therefore building structures are influential and considered a factor in numerical analysis.

**5.3 Subsoil Settlement**

To monitor the subsurface settlements, one borehole extensometer is placed above the tunnel center line (Fig. 3). The magnitude of subsurface settlement obtained after a three-month pass of TBM gradually increases toward the crown of the tunnel as shown in Fig. 10. This figure also show a good agreement between field measured data and numerical results.

When building structures are ignored from the analysis model, the results of the subsurface settlements are underestimated except for a deeper depth (beyond -20 m) where the effect of structures and their surcharge is negligible (Fig.10). Therefore, building structures must be considered in the input model.

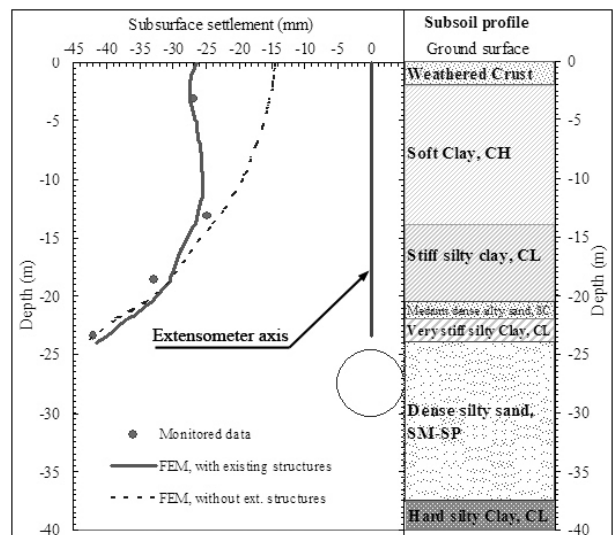


Fig. 10 Subsurface settlements along Extensometer ME-1

**6. Bridge and Building Displacements**

The settlements of the old Klongtan bridge pile foundations, where the TBM passes about 3 meters underneath, are recorded before, during and after the pass of EPB shield machine. However, the foundations in the canal are beyond the scope of this study. Except for the shield length, where the significant settlements are also observed, the behaviors of the bridge foundation settlements (Fig. 11) are very similar to those of the ground movements described previously. The settlements almost

stopped one week after the TBM passed (108 m) as well.

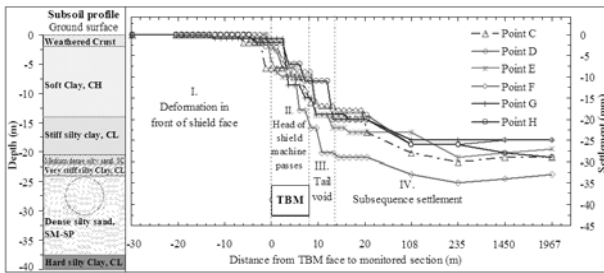


Fig. 11 Settlements of Klongtan bridge foundations in response to EPB tunneling

In addition to the old bridge, some building settlement points are also placed to monitor the settlements of 3- and 4-storey shophouses, which are located on the right side of the bridge (Fig. 2). The analysis configurations of each bridge foundation and the existing shophouses based on 2D FEM are the same whereas only the positions of the structures to the tunnel center line are adjusted according to the real analysis sections. The magnitudes of old bridge and shophouse settlements are listed in Table 2. The 2D-FEM results are well comparable with the monitored data.

Table 2 Magnitude of structure settlements

| Structure          | Source of data | Magnitude of settlement points |                |                |                |       |       |
|--------------------|----------------|--------------------------------|----------------|----------------|----------------|-------|-------|
|                    |                | C                              | D              | E              | F              | G     | H     |
| Bridge foundation  | Monitored data | -29                            | -34            | -28            | -25            | -25   | -28   |
|                    | 2D-FEM results | -30.3                          | -30.8          | -29.9          | -25.9          | -24.1 | -28.2 |
| 3-storey shophouse |                | C <sub>1</sub>                 | C <sub>2</sub> | C <sub>3</sub> | C <sub>4</sub> |       |       |
|                    | Monitored data | -2                             | -11            | -13            | -15            |       |       |
|                    | 2D-FEM results | -1.6                           | -9.8           | -12.2          | -16.7          |       |       |
| 4-storey shophouse |                | D <sub>1</sub>                 | D <sub>2</sub> | D <sub>3</sub> | D <sub>4</sub> |       |       |
|                    | Monitored data | -19                            | -22            | -15            | -5             |       |       |
|                    | 2D-FEM results | -17                            | -17.8          | -17.3          | -3.09          |       |       |

The parametric studies have been confirmed that the ratios of soil stiffness over the undrained shear strength ( $E_u/S_u$ ) are 240 and 480 for soft and stiff clays respectively. In addition, the  $E'$  ( $\text{kN/m}^2$ ) =  $2000.N_{60}$  for medium and dense silty sand layers have been confirmed in this research study as well.

## 7. Conclusions

Field monitored data are collected for performing empirical method and 2D FEM analyses. FEM analyses yield similar results to the field monitored data at the ground surface and subsurface settlements. The empirical method for surface settlements is also in agreement with the field monitored data and FEM analyses. When building structures above the site of the tunnel are included as a parameter of the analysis model, the results of the FEM are similar to those of the field monitored data. Thus, building structures have an influence on the soil movements. If the building structure was excluded, the settlements are underestimated. Elasto-plastic failure criteria of Mohr Coulomb soil model can be satisfactorily used for back simulation of the ground surface and subsurface movements caused by tunnel excavation. EPB shield bores the tunnel in dense silty sand layer about 27.5 m below ground surface. Consequently, an accurate prediction could be well made based on the back analysis of the case studies from the previous tunnel projects performed in similar geological conditions and included important parameters, e.g., building structures in their analyses.

## Acknowledgment

The authors are grateful to the following individuals: JICA and AUN/Seed-Net for funding this research, Dr. Sangrawee CHAOPRICHA for her review of the paper and useful suggestion and comments, the Bangkok Metropolitan Authority which owns this project for the permission to access to data collection, the staff of Italian Thai and Nishimatsu joint venture for providing the necessary monitored data and last but not least, SECC's staff and colleagues for their help during the initial setting analysis model.

## References

- [1] BRINKGREVE, R. B. J., "PLAXIS, Finite element code for soil and rock analyses, 2D-Version 8", A. A. Balkema, Rotterdam, Netherlands, 2002.

- [2] Karakus, M. and Fowell, R.J., "Back analysis for tunnelling induced ground movements and stress redistribution", *Tunnelling and Underground Space Technology*, Vol. 20, No. 6, 2005, pp. 514-524.
- [3] Mair, R. J., "Development in geotechnical research: Application to tunnels and deep excavations", *The unwin Memorial Lecture 1992, Proceedings of the Institution of Civil Engineers and Civil Engineering*, 1993, pp. 27-41.
- [4] Peck, R. B., "Deep excavations and tunneling in soft ground", *Proceedings of the 7<sup>th</sup> International Conference on Soil Mechanics and Foundation Engineering, State of the Art Volume*, Mexico City, 1969, pp. 225-290.
- [5] Phienwej, N., Sirivachiraporn, A., Timpong, S., Tavaratum, S. and Suwansawat, S., "Characteristics of Ground Movements from Shield Tunnelling of the First Bangkok Subway Line", *Proceedings of the International Symposium on Underground Excavation and Tunnelling, Urban Tunnel Construction for Protection of Environment*, Bangkok, Thailand, 2006, pp. 319-330.
- [6] Shibuya, S., Tamrakar, S.B. and Theramast, N., "Geotechnical Site Characterization on Engineering Properties of Bangkok Clay", *Journal of the Southeast Asian Geotechnical Society*, Vol. 32, No. 3, 2001, pp. 139-151.
- [7] Shibuya, S. and Tamrakar, S.B., "Engineering properties of Bangkok clay", *Proceedings International Symposium on Characterisation and Engineering properties of Natural Soils*, Singapore, Vol. 1, 2003, pp. 645-692.
- [8] Teeparaksa, W. and Heidengren, C. R., "Geotechnical aspects of the design and construction of the MRTA initial system project - The Bangkok Subway", *Journal of Society of Professional Engineers, Thailand*, No. 24 (Nov. 1998 - Nov. 1999), pp. 21-34.
- [9] Teeparaksa, W., "FEM Analysis of EPB Tunnelling Bored Underneath Through Underground Obstruction", *Proceedings of the 31<sup>st</sup> ITA-AITES World Tunnel Congress on Underground Space Use, Analysis of the Past and Lessons for the Future*, Istanbul, Turkey, Vol. 2, 2005, pp. 883-888.
- [10] Teeparaksa, W., Photayanuvat, C., Boonsong C. and Boonard, J., "Design of Subway Tunnel under the Chao Phraya River for Bangkok South Blue Line Extension", *Proceedings of International Symposium on Underground Excavation and Tunnelling, Urban Tunnel Construction for Protection of Environment*, Bangkok, Thailand, 2006, pp. 181-189.
- [11] Vermeer, P.A., Bonnier, P.G. and Moler, S.C., "On a Smart Use of 3D-FEM in Tunnelling", *Proceedings of the 8<sup>th</sup> international Symposium on Numerical Models in Geomechanics*, Rom, Italy, 2002, pp. 361-366.
- [12] Yeow, H.C., Gaba, A.R. and Pillai, A.K., "Concurrent Tunnelling and Station Excavation at Bangkok MRTA North", *Proceedings of the 15<sup>th</sup> Southeast Asian Geotechnical Society Conference*, Bangkok, Vol. 1, 2004, pp. 753-758.